

**Security Related Sensitive
Information
has been Redacted from the
Following Document**



Department of Mechanical and
Nuclear Engineering
302 Rathbone Hall
Manhattan, KS 66506 -5205
785-532-5610
Fax: 785-532-7057

P. Michael Whaley
Kansas State University
Nuclear Reactor Facilities Manager
112 Ward Hall
Manhattan, Kansas 66506

Daniel E. Hughes, Project Manager
Research and Test Reactors Section
New, Research and Test Reactors Program
Division of Regulatory Improvement Programs
Office of Nuclear Reactor Regulation

DATE: 20 March 2006

SUBJECT: Update to the Proposed Safety Analysis Report for the Kansas State
University TRIGA Mark II Nuclear Research Reactor

Dear Mr. Hughes:

A license renewal request was submitted for the Kansas State University in 2002, and the facility is currently operating under "timely renewal" provisions. USNRC review has resulted in Requests for Additional Information (RAI), previously addressed; further clarification is provided in the attached and revised Chapter 13 of the proposed Safety Analysis Report.

This revision incorporates two changes in analysis and some editorial changes. The analysis of postulated loss of pool water was performed using a more detailed MCNP5 model. The source term for the maximum hypothetical accident was revised for 1,250 kW operations. In addition, there are editorial revisions in Section 13.1, and the equation numbering format was revised to be consistent with Chapter 4.

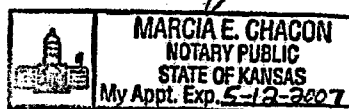
If you have any questions or comments concerning this matter, you may contact me at 785-532-6657 or whaley@ksu.edu.

I verify under penalty of perjury that the foregoing is true and correct,

Executed on 20 March 2006,


P. M. Whaley

Docket No. 50-188
Enclosures: as indicated



Marcia E Chacon
3-20-2006

13. ACCIDENT ANALYSIS

This chapter provides information and analysis to demonstrate that the health and safety of the public and workers are protected in the event of equipment malfunctions or other abnormalities in reactor behavior. The analysis demonstrates that facility design features, limiting safety system settings, and limiting conditions for operation ensure that no credible accident could lead to unacceptable radiological consequences to people or the environment.

13.1 Accident Initiating Events and Scenarios

There are three accident scenarios in the initial licensing of the K-State Reactor Facility in 1962 for 100-kW steady-state operation and in the 1968 upgrade of the license permitting 250-kW steady state operation with 250-MW pulsing operation. The current analysis presented below considers the same scenarios, but for steady-state operation at 1,250 kW and pulsing operation to a \$3.00 reactivity insertion with an estimated peak power of 1,340 MW.

This chapter deals with analysis of abnormal operating conditions and consequent effects on safety to the reactor, the public, and operations personnel. The three scenarios analyzed are:

- Loss of coolant
- Insertion of excess reactivity
- Fuel encapsulation failure — the maximum hypothetical accident (MHA)

A loss of coolant accident is analyzed to demonstrate that maximum fuel temperature does not exceed acceptable limits. Dose from scattered radiation from the uncovered core is also analyzed.

Insertion of excess reactivity is considered for two sets of initial conditions. First, the maximum reactivity addition from operations below feedback range is considered with respect to maximum fuel temperature. Since the pulse increases fuel temperature from the initial condition, operation at power is assumed prior to pulsing; with the reactor operating at power with a corresponding elevation in fuel temperature, reactivity available for pulsing is reduced.

The maximum hypothetical accident for a TRIGA reactor is the failure of the encapsulation of one fuel element, in air, resulting in the release of airborne and gaseous fission products to the atmosphere. Failure in air could result from a fuel-handling accident or, possibly, failure in the event of a loss of reactor coolant. Failure under water, leading ultimately to atmospheric release of fission products, could possibly result from insertion of excess reactivity or operation with damaged fuel. This chapter addresses the several scenarios potentially leading to fuel failure, and then the potential consequences, should failure occur in air.

13.2 Accident Analysis and Determination of Consequences

13.2.1 Notation and Fuel Properties

Tables 13.1-13.3 identify physical characteristics of the TRIGA Mark II fuel. Table 13.4 identifies the assumptions and design basis values used in the accident analyses.

Table 13.1, Dimensions of TRIGA MkII ZrH_{1.6} Fuel Elements.

Property of Individual Element	Symbol	Value
Length of fuel zone	L_f	[REDACTED]
Fuel radius	r_i	[REDACTED]
Clad outside radius	r_o	[REDACTED]
Fuel volume	V_f	[REDACTED]
Clad volume	V_c	[REDACTED]
Fuel mass	M_f	[REDACTED]
Clad mass	M_c	[REDACTED]
Wt. Fraction U in fuel	x_u	[REDACTED]
Wt. Fraction ZrH _{1.6} in fuel	x_m	[REDACTED]

Source: [REDACTED]

Table 13.2. Neutronic Properties of TRIGA MkII ZrH_{1.6} Fuel Elements.

Property	Symbol	Value
Effective delayed neutron fractions	β	0.007
Effective neutron lifetime	ℓ	43 μ sec
Temperature coefficient of reactivity	α	-0.000115 K ⁻¹

Source: [REDACTED]

Table 13.3, Thermal and Mechanical Properties of TRIGA MkII ZrH_{1.6} Fuel Elements and Type 304 Stainless Steel Cladding.

Property	Symbol	Value	Temp.
<i>Fuel</i>			
Density	ρ_f	[REDACTED]	
Thermal conductivity	k_f	[REDACTED]	All
Heat capacity, $c_{pf} = 340.1 + 0.6952T(^{\circ}\text{C})$	c_{pf}	[REDACTED]	0 $^{\circ}\text{C}$
<i>Cladding</i>			
Density	ρ_c	[REDACTED]	300 K
Thermal conductivity	k_c	14.9 W m ⁻¹ K ⁻¹	300 K
		16.6	400 K
		19.8	600 K
Heat capacity	c_{pc}	477 J kg ⁻¹ K ⁻¹	300 K
		515	400 K
Yield strength		250 Mpa	400 $^{\circ}\text{C}$
Tensile strength		455 Mpa	400 $^{\circ}\text{C}$

Source: [REDACTED]; cladding properties from Incropera and DeWitt (1990) and from Metals Handbook (1961).

Table 13.4, KSU TRIGA Core-Conditions Basis for Calculations.

Steady state maximum power, P_0	1,250 kW
Fuel mass per element	[REDACTED]
Heat capacity per element at T (°C)	[REDACTED]
Minimum number of fuel elements, N	[REDACTED]
Core radial peaking factor	2
Axial peaking factor	$\pi/2$
Excess reactivity	\$4.00 (2.8% $\Delta k/k$)
Maximum pulsing reactivity insertion	\$3.00 (2.1% $\Delta k/k$)
Excess reactivity at [REDACTED] maximum power ^a	\$1.16 (0.81% $\Delta k/k$)
Fuel average temperature at [REDACTED] maximum power ^a	285 °C

^aSource: Data from GA Tofrey Pines TRIGA reactor

13.2.2 Loss of Reactor Coolant

Although total loss of reactor pool water is considered to be an extremely improbable event, calculations have been made to determine the maximum fuel temperature rise that could be expected to result from such an event taking place after long-term operation at full power of 500 kW. Limiting design basis parameters and values are addressed by Simnad (1980) as follows:

Fuel-moderator temperature is the basic limit of TRIGA reactor operation. This limit stems from the out-gassing of hydrogen from the ZrH_x and the subsequent stress produced in the fuel element clad material. The strength of the clad as a function of temperature can set the upper limit on the fuel temperature. A fuel temperature safety limit of 1150°C for pulsing, stainless steel U-ZrH_{1.65} ... fuel is used as a design value to preclude the loss of clad integrity when the clad temperature is below 500°C. When clad temperatures can equal the fuel temperature, the fuel temperature limit is 950°C. There is also a steady-state operational fuel temperature design limit of 750°C based on consideration of irradiation- and fission-product-induced fuel growth and deformation...

This section demonstrates under extraordinarily conservative assumptions that maximum fuel temperature reached in a loss of coolant accident is well below any safety limit for TRIGA reactor fuel. Conservatism notwithstanding, the margin between computed temperature and design limits is sufficiently great to accommodate a design margin of at least a factor of two.

a. Initial Conditions, Assumptions, and Approximations

The following conditions establish the scenario for analysis of the loss of coolant accident.

- The reactor is assumed to have been operating for infinite time at power $P_0 = 1,250$ kW at the time coolant is lost.
- Coolant loss is assumed to be instantaneous.
- Reactor scram is assumed to occur simultaneously with coolant loss.
- Decay heat is from fission product gamma and x rays, beta particles, and electrons. Effects of delayed neutrons are neglected.
- Thermal power is distributed among [REDACTED] fuel elements, with a radial peak-to-average ratio of 2.0. In individual elements, thermal power is distributed axially according to a sinusoidal function.

- Cladding and gap resistance are assumed to be negligible, i.e., cladding temperature is assumed to be equal to the temperature at the outside surface of the fuel matrix.
- Cooling of the fuel occurs via natural convection to air at inlet temperature $T_i = 300^\circ\text{K}$. Radiative cooling and conduction to the grid plates are neglected.
- Heat transfer in the fuel is one dimensional, i.e., axial conduction is neglected, and fuel is assumed to be uniform in thermophysical properties.
- Heat transfer in the fuel is treated as pseudo-steady-state behavior, i.e., at any one instant, heat transfer is described by steady-state conduction and convection equations.¹

b. Core Geometry

The following data on core geometry are derived from the KSU TRIGA Mechanical Maintenance and Operating Manual (1962). The core contains fuel positions in five circular rings (B - F), plus the central thimble (A ring). The upper grid plate is 0.495 m in diameter and 0.019 m thick. Holes to position the fuel are 0.03823 m diameter and the central thimble is very slightly larger in diameter, 0.0384 m.

Cooling water passes through the differential area between the triangular spacer block on the top of each fuel element and the round holes in the upper grid plate. The nominal diametral clearance between the tips of the spacer blocks and the grid plate is approximately 0.001 m.

The lower grid plate is 0.405 m diameter, with 36 holes, 0.0159 m diameter, for water flow. However, the bulk of the water flow is through the annular space provided between the top of the lower grid plate and the bottom of the reflector. The radial reflector is $D_r = 0.457$ m inside diameter and 0.559 m height.

With an experiment in the central thimble, effective hydraulic diameter for core flow is:

$$D_h = \frac{4 * A_{flow}}{P_{wet}} = \frac{4 * (\frac{\pi * D_r^2}{4} - \pi * r^2)}{\pi * D_r + 2 * \pi * r_0} = 0.02127m \quad (1)$$

If, in thermal-hydraulic calculations, one approximates conditions as flow through an annular section around any one fuel element, the outer radius of the annulus, say r_o , is given by

$$D_h = \frac{4\pi(r_o^2 - r_c^2)}{2\pi r_o}, \text{ or} \quad (2)$$

$$r_o = \sqrt{D_h r_c / 2 + r_c^2} = \text{m,}$$

The flow area A_c per fuel rod is $\pi(r_o^2 - r_c^2) = \pi r_o D_h / 2 = \text{m}^2$.

The total length of a fuel rod is , of which the length of the fuel matrix, the heated length, is . The lengths of upper and lower axial reflectors, L_u

¹ See Todreas & Kazemi (1990) or El-Wakil (1971) for steady-state conduction equations.

and L_i , are each [redacted]. Beneath the lower reflector is a bottom end fixture of length L_i about [redacted]. Above the upper reflector is a triangular spacer of length L_i about [redacted] and an upper end fitting of length L_u about [redacted]. The zone between grid plates is $L_z = L_i + L_i + L_f + L_u =$ [redacted]

c. Decay Power

The time dependence of the thermal power in the core as a function of time after shutdown is based on calculations by the CINDER code [England et al. 1976] as reported by George, LaBauve, and England [1980, 1982]. Sample results are presented in figure 13.1 and Table 13.5 as the function $R(t)$ defined as the ratio of the thermal power $P_d(t)$ from gamma ray and beta particle decay at time t after shutdown to the steady power P_o prior to shutdown, based on 200 MeV energy release per fission.

For the purpose of this analysis, the time dependence function for 1 to 10^6 s may be approximated as

$$R(t) = \frac{0.04856 + 0.1189x - 0.0103x^2 + 0.000228x^3}{1 + 2.5481x - 0.19632x^2 + 0.05417x^3}, \tag{3}$$

in which x is the natural log of the time after shutdown, in seconds. Time dependence of the thermal source in the worst-case element is given by

$$P_d(t) = \frac{2P_o}{N} R(t), \tag{4}$$

in which the worst case element generates twice the power as the core average, P_o is the total-core thermal power prior to shutdown (1,250 kW), and N [redacted] is the minimum number of fuel elements required for operation.

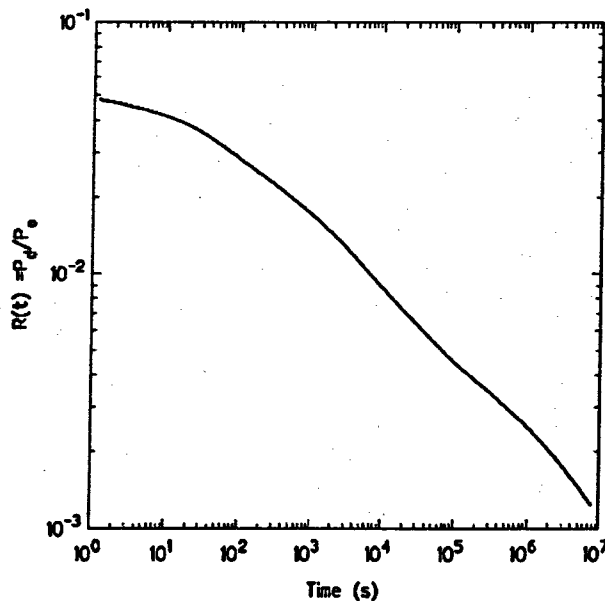


Figure 13.1. Decay Heat Function $R(t)$.

Table 13.5, Decay Heat Function for Thermal Fission of ^{235}U .

Time t (s)	$R(t) = P_d(t)/P_o$
0	0.0526
1 (10^0)	0.0486
10 (10^1)	0.0418
100 (10^2)	0.0282
1000 (10^3)	0.0172
10,000 (10^4)	0.0087
100,000 (10^5)	0.0044
1,000,000 (10^6)	0.0025

d. Maximum Air Temperature

The fundamental relationships between buoyancy driven differential pressure and pressure losses from friction provide an independent verification for results of the previous calculations.

Buoyancy Driven Pressure Difference

The total mass flow rate w (kg/s) associated with the worst-case fuel element is determined by a balance between the buoyancy driven pressure difference vertically across the core and the frictional pressure loss within the core, which is discussed in the next section. The temperature rise across the core is

$$\Delta T_m(t) = T_o(t) - T_i = \frac{P_d(t)}{wc_{pm}^{air}} = \frac{2P_o R(t)}{Nwc_{pm}^{air}}, \quad (5)$$

in which the heat capacity of the air evaluated at the inlet air temperature. At time zero, for example,

$$\Delta T_m(0) = T_o(0) - T_i \cong 0.6153 / w. \quad (6)$$

Air inlet temperature T_i is assumed to remain constant at 27°C. Suppose ρ_i and ρ_o are respectively the densities of air at the inlet and outlet temperatures.² Suppose further that the effective chimney height is H . The chimney height is the distance between the center of the zone in which the air is heated and the center of the zone in which the air is cooled. Evaluation of the latter is difficult to determine because of uncertainties in mixing of the air after it leaves the upper grid plate. Here we follow the lead of the UT SAR (1991) and choose 10 hydraulic diameters as the effective distance. Thus, H is given by $L_f/2 + L_i + 10D_h$ and the buoyancy pressure difference is given by

$$\Delta p_b = (\rho_i - \rho_o) * g * H \quad (7)$$

in which g is the acceleration of gravity, 9.8 m s⁻². Since

$$\rho_i - \rho_o \cong \frac{353 * (T_o - T_i)}{T_i^2}, \quad (8)$$

² Density at 1 atm, for air as an ideal gas, is given by ρ (kg/m³) = 353.0/T(°K). Heat capacity, from 300 to 700 °K is 1030 J/kgK ± 3% (Incropera and DeWitt, 1990).

and $T_i = 300$ K, it follows from Eqs. (5) and (8) that

$$\Delta p_b(t) = 0.190R(t) / w, \tag{9}$$

Frictional Pressure Difference

In this calculation, only frictional losses within the core, computed on the basis of the equivalent annulus model, are accounted for. Based on air inlet density and an air mass flow rate per fuel rod of w , the frictional pressure difference is given by

$$\Delta p_f = \frac{L_c f w^2}{2 \rho_i D_h A_c^2}. \tag{10}$$

The laminar-flow (Moody) friction factor f for the equivalent annulus model, with $r_o / r_i = 1.193$ is given by Sparrow and Loeffler (1959) as

$$f = 100 / Re, \tag{11}$$

Re, the Reynolds number, is given by $D_h w / \mu_i A_c$, and μ_i is the dynamic viscosity of the air at the inlet temperature.³ Equation (10) may be rewritten as

$$\Delta p_f = \frac{0.1416 L_c \mu_i T_i w}{D_h^2 A_c} = 1780w, \tag{12}$$

Equating the frictional pressure drop with the buoyancy pressure driving force, using Equations (9) and (12),

$$w = 0.0103 \sqrt{R(t)}, \tag{13}$$

or

$$T_o(t) - T_i = \Delta T(t) = 1140 \sqrt{R(t)}. \tag{14}$$

Results

For $R(t)$ at time zero of 0.0526, maximum air temperature rise above 300 K is 261 K.

e. Fuel and Cladding Temperature Distribution

With design power $P_o = 1,250$ kW, a factor of two radial peak to average power, and a fuel surface area in the heated zone equal to $A_f = 2\pi r_o L_f$, the worst-case average heat flux at post-accident time t in the heated zone is:

$$q''_{max} = 2 * 1.25e6 * R(t) / A_f N = \dots W/m^2. \tag{15}$$

With the conservative approximation that the axial variation of heat flux is sinusoidal, the local value of the heat flux (W/m^2) is given by:

$$q''(z) = q''_{max} \sin(\pi z / L_f), \tag{16}$$

³ Dynamic viscosity, over the range 250 - 1000 °K is given by $10^7 \mu$ (Ns/m²) = -106.2941 + 16.81986[T(°K)]^{1/2} or $\mu = 1.85 \times 10^{-5}$ Ns/m² at 300 °K. (Incropera and DeWitt, 1990).

in which z is the distance along the fuel channel, measured from the inlet and $q''_{\max} = (\pi/2)q''_{\text{avg}} = 4.235 \times 10^5 R(t) \text{ W/m}^2$. Similarly, the local value of the air temperature in the coolant channel is given by

$$T_{\text{air}}(z) = T_i + \frac{0.6153R(t)}{2} [1 - \cos(\pi z / L_f)] \quad (17)$$

According to Dwyer and Berry (1970), the Nusselt number for laminar flow in a cooling channel is approximately $\text{Nu} = 4.24$. The corresponding heat transfer coefficient is

$$h = \frac{k_{\text{air}} \text{Nu}}{D_h} \quad (18)$$

By using as an approximation the air thermal conductivity⁴ of 26.3 W/mK at 300°K, one computes $h = 5240 \text{ W/m}^2\text{K}$, and the cladding surface temperature

$$T_{\text{clad}}(z) = T_{\text{air}}(z) + q''(z) / h \quad (19)$$

By using the fuel thermal conductivity $k_f = 18 \text{ W/mK}$, and neglecting the temperature drop across the cladding, one computes the fuel centerline temperature as

$$T_{\text{fuel}}(z) = T_{\text{clad}}(z) + \frac{q''(z)r_o}{2k_f} \quad (20)$$

Fuel and cladding temperatures are reported in Table 13.6 and illustrated in figure 13.2 for the case of zero time post accident. This is based on three conservative assumptions: equilibrium fission product buildup at full power, instantaneous loss of coolant when the reactor scram occurs, and equilibrium temperature based on initial decay heat production.

Table 13.6, Post-Accident Fuel and Cladding Temperatures.

z/L_f	$q'' \text{ (W/m}^2\text{)}$	$T_{\text{air}} \text{ (}^\circ\text{K)}$	$T_{\text{clad}} \text{ (}^\circ\text{K)}$	$T_{\text{fuel}} \text{ (}^\circ\text{K)}$
0.00	0	300	300	300
0.10	17209	306	309	318
0.20	32733	325	331	348
0.30	45053	354	362	385
0.40	52963	390	400	427
0.50	55688	431	441	470
0.60	52963	471	481	508
0.70	45053	508	516	539
0.80	32733	536	542	559
0.90	17209	555	558	567
1.00	0	561	561	561

⁴ For the range 200 to 1000°K, data of Incropera and DeWitt (1990) is very well fit by the formula $k_{\text{air}} = -22.055 + 2.8057\sqrt{T(\text{K})}$ in units of W/mK.

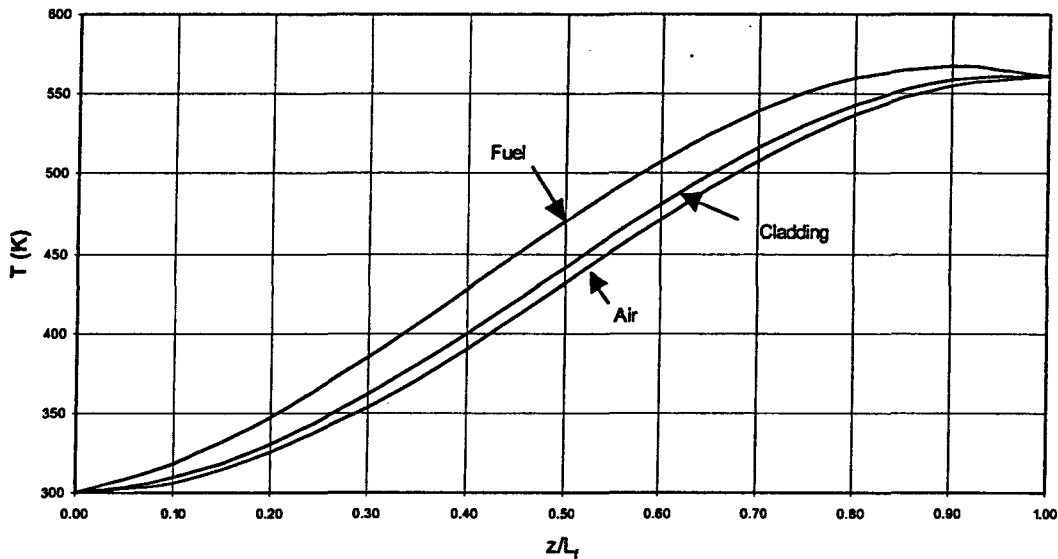


Figure 13.2, Axial Variation of fuel, cladding, and air temperature immediately following a loss of coolant accident, with equilibrium fission product heating.

Any conceivable period of operations has significantly lower power generation than the assumed power history, and total inventory of fission products is significantly lower than the assumed value. During actual loss of coolant, overall heat transfer coefficient will be based on water rather than air. There is at least 16 feet of water over the core that has to drain before the core is uncovered. Experiments reported in GA-6596 "Simulated Loss-of-Coolant Accident for TRIGA Reactors" (General Atomics, August 18, 1965) demonstrated that with a constant and continuous heat production, temperature rises to about 50% of the equilibrium temperature in approximately 30 minutes (1800 seconds). At 10^3 seconds, $R(t)$ is 0.0172, 33% of the heat production following shutdown. Equilibration takes a significant amount of time, while heat production is decaying. Although the analysis assumptions are extremely conservative, calculations show a wide margin to limiting temperatures.

f. Radiation Levels from the Uncovered Core

Although there is only a very remote possibility that the primary coolant and reactor shielding water will be totally lost, direct and scattered dose rates from an uncovered core following 1,250 kW operations are calculated.

This section describes calculations of on-site and off-site radiological consequences of the loss-of-coolant accident. Extremely conservative assumptions are made in the calculations, namely, operation at 1,250 kW for one year followed by instant and simultaneous shutdown and loss of coolant. Gamma-ray source strengths, by energy group, are determined by ORIGEN-2 [CCC-371] as shown in Table 13.7. Radiation transport calculations are performed using the MCNP code. Calculations were performed using a 1270 cm boundary for doses inside the reactor bay, and 12000 cm for doses outside the reactor bay.

Table 13.7, Full Core Gamma-Ray Sources Strengths (Number Per Second) Following Operation for One Year at 1,250 kW Thermal Power.

E (MeV)	Time after shutdown				
	0	1 h	24 h	30 days	180 days
1.00E-02	8.72E+	2.92E+	1.05E+	2.43E+	6.20E+
2.50E-02	2.09E+	7.50E+	3.04E+	5.97E+	1.32E+
3.75E-02	1.74E+	7.37E+	3.97E+	6.72E+	1.45E+
5.75E-02	1.81E+	5.50E+	1.77E+	4.15E+	1.20E+
8.50E-02	1.50E+	5.20E+	2.33E+	3.21E+	8.39E+
1.25E-01	1.50E+	7.65E+	4.81E+	8.98E+	1.31E+
2.25E-01	3.11E+	1.03E+	4.44E+	2.42E+	6.83E+
3.75E-01	1.94E+	5.72E+	2.20E+	3.81E+	3.41E+
5.75E-01	3.25E+	1.71E+	7.54E+	1.01E+	1.08E+
8.50E-01	4.16E+	2.26E+	8.94E+	4.51E+	1.15E+
1.25E+00	2.22E+	8.15E+	7.83E+	1.62E+	6.01E+
1.75E+00	9.30E+	5.14E+	2.23E+	4.78E+	7.72E+
2.25E+00	5.00E+	2.19E+	6.69E+	1.12E+	3.72E+
2.75E+00	1.99E+	7.32E+	8.13E+	1.82E+	1.55E+
3.50E+00	1.16E+	1.72E+	7.12E+	1.50E+	9.37E+
5.00E+00	6.23E+	2.42E+	6.96E+	4.67E+	4.63E+
7.00E+00	5.05E+	5.27E+	5.27E+	5.26E+	5.22E+
9.50E+00	9.49E+	5.98E+	5.98E+	5.98E+	5.93E+
Total	3.39E+	1.35E+	5.27E+	1.20E+	2.61E+
MeV/s	1.43E+	6.28E+	2.02E+	5.77E+	1.13E+

Modeling of the reactor core for radiation transport calculations using the MCNP code (Appendix A) incorporates was performed using approximate geometry described in figures 13.4 and 13.4. The TRIGA reactor core is approximated as a right circular cylinder [redacted] diameter (OD of F ring). The fuel region is [redacted] high. On each end axially is a graphite zone [redacted] high and an aluminum grid plate [redacted] thick. In [redacted] fuel locations, there are [redacted] fuel elements, [redacted] standard control rods and [redacted] transient control rod, 1 void location, 1 central thimble (void), 1 source (assume void), and 1 pneumatic transfer site (assume void). The fuel region is treated as a homogeneous zone, as are the axial graphite zones and the grid plates.

Biological shielding is approximated as a two-section concrete cylinder, approximately [redacted] feet [redacted] thick at the bottom and reduced to [redacted] feet [redacted] at the [redacted] foot [redacted] elevation as shown in figure 13.3. The control rod drives are positioned on a ¼ in. (1.905 cm) steel bridge-plate, supported by structural steel members; the bridge-plate is modeled.

The core is modeled conservatively as a central homogenous fuel zone (air density neglected) bounded on either end by a homogeneous axial reflector zone and a 0.75-in. (1.905 cm) thick aluminum grid plate treated as a homogeneous solid. The source is assumed to be uniformly distributed within the core.

Homogenization of the fuel region is based on averaging fuel geometry and materials over the core volume. Fuel elements are [redacted], clad with type 304 stainless

steel⁵. Fuel density is [REDACTED]. Fuel composition is 8.5% uranium, 91.4% ZrH_{1.65}. The uranium is 20% ²³⁵U and 80% ²³⁸U. Steel density is 7900 kg/m³. Standard control rods are [REDACTED] OD, the transient rod [REDACTED] OD. Both types of rods are clad with 30-mil thick aluminum (2700 kg/m³ density). The control material may be approximated as pure graphite, with density 1700 kg/m³.

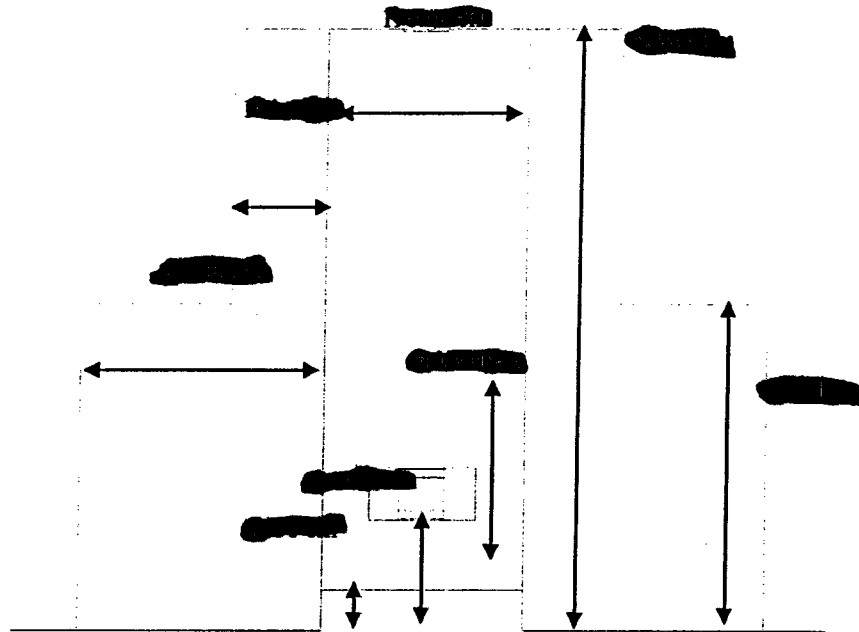


Figure 13.3, Core and Biological Shielding MCNP Model

Densities of the homogenous zones are as follow:

Fuel	[REDACTED]
Reflector	1147 kg/m ³
Grid Plate	2700 kg/m ³

Composition of the three zones, by weight fraction, are given in Table 13.8.

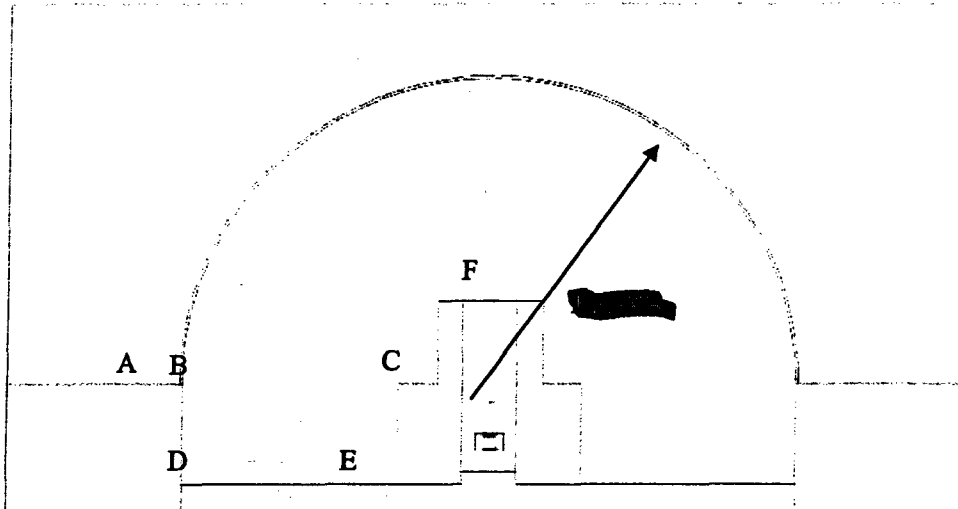
Table 13.8, Compositions of Homogenized Core Zones.

Element	Mass Fraction	Element	Mass Fraction
<i>Fuel Zone</i>		<i>Axial Reflector Zone</i>	
C	0.0617	C	0.7920
Al	0.0010	Al	0.0033
H	0.0139	Mn	0.0041
Zr	0.7841	Cr	0.0368
Mn	0.0013	Ni	0.0164
Cr	0.0117	Fe	0.1474
Ni	0.0052	<i>Grid Plate</i>	
Fe	0.0469	Al	1.0000
U	0.0741		

The

⁵ Composition, by weight, 2% Mn, 18% Cr, 8% Ni, balance Fe.

reactor bay is approximated as a hemispherical dome (illustrated in figure 13.4) covering a right circular cylinder [redacted] high and [redacted] radius, with the dome 10 cm thick. The reactor bay free volume is [redacted]. The site boundary, at its nearest approach to the reactor bay, is about 2 m beyond the bay boundary, at a radius of [redacted] from the center of the reactor. Receptor locations within the reactor bay were selected 30 cm from vertical surfaces, 100 cm from horizontal surfaces. Receptor locations outside the reactor bay include the radius of the controlled area (fence around the reactor bay), 20 m, 30 m, 40 m, 50 m, 70 m and 100 m.



Key	Receptor Location	Radius	Elevation
		Meters	Meters
A	2 meters beyond dome (radius of controlled area)	[redacted]	[redacted]
B	1 meter above grade/12-foot level 30 cm inside the dome	[redacted]	[redacted]
C	1 meter above 12-foot working platform 30 cm from biological shielding	[redacted]	[redacted]
D	1 meter above the reactor bay floor, 30 cm from the wall	[redacted]	[redacted]
E	1 meter above the reactor bay floor, 30 cm from the biological shielding	[redacted]	[redacted]
F	1 meter above the 22-foot level, reactor center	[redacted]	[redacted]

Figure 13.4, Reactor Bay MCNP Model

The roof of the reactor bay is modeled as a concrete slab 10 cm thick, density 2.35 g/cm³. The reactor bay confinement dome is actually a complex structure of composite material pinned to structural steel web and covered with aluminum for protection from the elements. As shown in figure 13.5, structural material is more concentrated at the peak of the dome except for a central aperture where the exhaust fan is mounted.

Dose rates at receptor locations following a loss of coolant accident are shown in Table 13.9. The 22-foot level is direct access to the reactor pool. [redacted]

[redacted] the reactor pool are located on the 0-foot level. Dose rates directly above the reactor tank void following 1,250 kW operations preclude occupancy, but dose rates on the 12 foot and 0 foot level would permit immediate occupancy over a considerable period time without exceeding occupational dose limits to undertake mitigating actions. The 13-meter distance marks a zone defined by the fence surrounding the reactor bay. Doses are calculated 1 meter above horizontal surfaces and 30 cm from vertical surfaces (i.e., for doses adjacent to biological shielding and reactor bay walls).



Figure 13.5, Confinement domes structure directly over the reactor pool

These dose rates are unrealistically conservative in view of the assumed full power operating history (not a physically possible scenario) scattered from a continuous concrete roof. Kansas State University has complete control over access to campus locations within the zones defined by receptor locations in the analysis.

Table 13.9, Gamma-Ray Ambient (Deep) Dose Rates (R/h) at Selected Locations for Times Following Loss of Coolant After Operation for One Year at 1,250 kW Thermal Power.

	Time post accident				
	0	1 h	24 h	30 d	180 d
<i>On-site elev.—elevation (radius from center of reactor bay/core)</i>					
22 ft. (center)	1.48E4	5.03E3	1.43E3	3.41E2	6.19E1
12 ft. (220.5 cm)	1.28E1	4.44E0	1.53E0	3.61E-1	7.49E-2
0 ft. (365.28 cm)	4.79E0	1.71E0	5.78E-1	1.38E-1	2.94E-2
12 ft. (1018 cm)	1.28E1	4.75E0	1.58E0	3.92E-1	8.16E-2
0 ft. (1018 cm)	1.09E1	3.90E0	1.28E0	3.18E-1	6.62E-2
<i>Off-site — radius from center of reactor bay/core</i>					
13.28 m	2.59E-1	2.97E-2	3.23E-2	8.70E-3	1.82E-3
20 m	1.15E-1	1.29E-2	1.35E-2	3.12E-3	6.13E-4
30 m	6.56E-2	7.10E-3	6.75E-3	1.87E-3	3.55E-4
40 m	4.59E-2	4.97E-3	5.13E-3	1.35E-3	2.36E-4
50 m	3.08E-2	3.56E-3	3.45E-3	8.37E-4	1.72E-4
70 m	1.98E-2	2.31E-3	2.01E-3	5.39E-4	1.06E-4
100 m	1.05E-2	1.25E-3	1.30E-3	3.05E-4	5.63E-5

g. Conclusions

Although a loss of pool water is considered to be an extremely improbable event, calculations show the maximum fuel temperature that could be expected to result from such an event (after long-term operation at full power of 1,250 kW) is 294°C, well below any safety limit for TRIGA reactor fuel.

Maximum possible dose rates resulting from a complete loss of pool water permit mitigating actions. The area surrounding the reactor is under control of the Kansas State University, and exposures outside the reactor bay environment can be limited by controlling access appropriately. Kansas State University has complete authority to control access to campus locations.

13.2.3 Insertion of Excess Reactivity

Rapid compensation of a reactivity insertion is the distinguishing design feature of the TRIGA reactor. Characteristics of a slow (ramp) reactivity insertion are less severe than a rapid transient since temperature feedback will occur rapidly enough to limit the maximum power achieved during the transient. Analyses of plausible accident scenarios reveal no challenges to safety limits for the TRIGA. The fuel-integrity safety limit, according to Simnad (1980), may be stated as follows:

Fuel-moderator temperature is the basic limit of TRIGA reactor operation. This limit stems from the out-gassing of hydrogen from the ZrH_x and the subsequent stress produced in the fuel element clad material. The strength of the clad as a function of temperature can set the upper limit on the fuel temperature. A fuel temperature safety limit of 1150°C for pulsing, stainless steel U-ZrH_{1.65} ... fuel is used as a design value to preclude the loss of clad integrity when the clad temperature is below 500°C. When clad temperatures can equal the fuel temperature, the fuel temperature limit is 950°C.

Two reactivity accident scenarios are presented. The first is the insertion of 2.1% reactivity at zero power by sudden removal of a control rod. The second is the sudden removal of the same reactivity with the core operating at the maximum power level permitted by the balance of the core excess reactivity (i.e., core excess less \$3.00). Movements of control rods for the first case are controlled, in part, administratively, while movements for the second are prevented by control circuit design.

As the analysis shows, in neither scenario does the peak fuel temperature approach the temperature limit. The nearest approach is 869°C, incurred by a pulse insertion of 0.7% while the reactor is operating at a steady power of 94 kW, an action prevented both by administrative requirements and by interlocks.

a. Initial Conditions, Assumptions, and Approximations

The following conditions establish an extremely conservative scenario for analysis of insertion of excess reactivity.

- The reactor operates with a minimum of $N =$ fuel rods.
- Reactor and coolant ambient (zero power) temperature is 27°C.
- Maximum reactivity insertion for pulsing or for the worth of experiments is set at \$3.00, $\delta k_{\max} = 2.1\%$ or $\rho_{\max} = 0.021$.

- Reactor power equivalent to the core excess reactivity of \$1.00, i.e., $\delta k = \delta k_{ex} - \delta k_{max} = 0.7\%$ ($\rho = 0.007$) is $P_o = 107$ kW and the maximum fuel temperature at that power is $T_o = 150^\circ\text{C}$. Basis: Data for the Torrey Pines TRIGA, as included in the KSU TRIGA Operations Manual.
- A control rod interlock preventing pulsing operations from power levels greater than a maximum of 10 kW is not credited
- Conservative hot channel factors as calculated in 4.5.3 are used

b. Computational Model for Power Excursions

The following relationships are for the Fuchs-Nordheim model, modified by Scalletar, for power excursions, as described for the TRIGA reactor by West et al. (1967).

If the heat capacity of the fuel is given by $c_{pf} = 340.1 + 0.6952T(^{\circ}\text{C})$ (J/kg $^{\circ}\text{K}$), and there are N fuel elements, each of mass m_f , then the overall core heat capacity is given by

$$K \text{ (J / K)} = m_f N c_{pf} = C_o + C_1 T(^{\circ}\text{C}) \tag{21}$$

in which $C_o = 6.682 \times 10^4$ and $C_1 = 136.6$. If P_o (W) is the reactor power at the initiation of the pulse power excursion, and ρ_o is the magnitude of an initiating step change in reactivity, then the maximum power increase (W) is given by

$$P_{max} - P_o = \frac{(\rho - \beta)^2 C_o}{2\alpha l} + \frac{(\rho - \beta)^3 C_1}{6\alpha^2 l} \tag{22}$$

A maximum pulse of \$3.00 would result in a power rise of approximately 1430 MW(t). If T_o is the average core temperature at the start of the excursion, the maximum temperature rise ($^{\circ}\text{K}$) is given by

$$T_{max} - T_o = \left[\frac{2 * (\rho - \beta)}{\alpha} \right] * \left[-\frac{3}{8} * (\sigma - 1) \pm \frac{3}{8} * \sqrt{(\sigma - 1)^2 + \frac{16}{3} * \sigma} \right] \tag{23}$$

in which

$$\sigma = \frac{\alpha C_o}{(\rho - \beta) C_1} \tag{24}$$

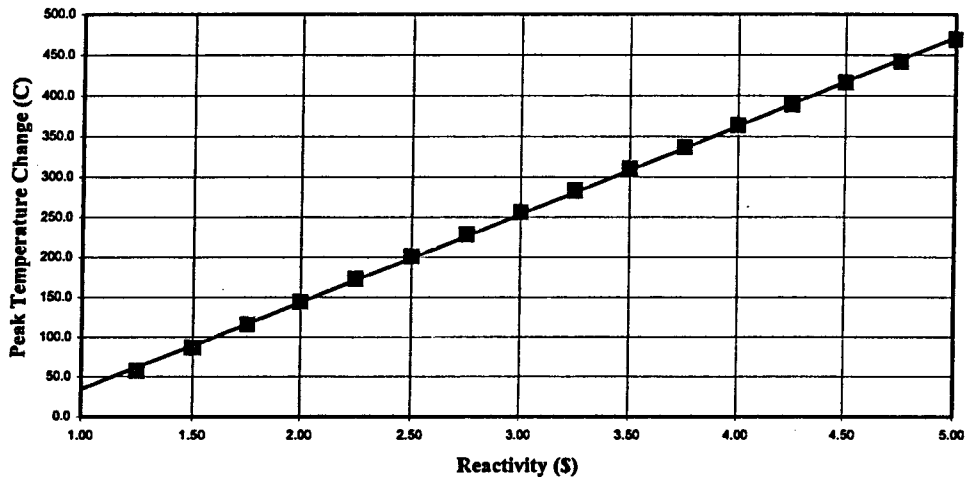
and the “+” sign applies when $\sigma > 1$. Although there are nonlinear terms in the model, calculation of temperature change as a function of temperature shows a nearly linear response. Therefore the major factor in determining core-average peak temperature is the amount of reactivity available to pulse. To remain within 1000°C at all locations, core average temperature cannot exceed 318°C (based on Table 13.4 peaking factors).

The maximum worth of the pulse rod is \$3.00, therefore peak temperature following a pulse was calculated based on a maximum reactivity available from the pulse rod at reference core temperature (27°C). The core-average temperature change is 229°C , with a hot spot change

of 716°C (based on Table 13.2.1.4 peaking factors). Therefore, core-average peak temperature for a \$3.00 pulse from 27°C is 256°C, with a hot spot temperature of 746°C.

With \$3.00 reserved for a maximum pulse, the reactor has remaining reactivity \$1.00 greater than critical to support operation at power. Reactivity of \$1.00 allows operation 94 kW; 94 kW operation results in an average fuel temperature of 48°C, and a hot-spot fuel temperature of 150°C. A \$3.00 pulse increases this hot spot temperature from 150°C to 869°C.

Change in Peak Temperature Versus Pulsed Reactivity



Fig

ure 13.3, Change in Peak Temperature Versus Pulsed Reactivity Insertion

The postulated scenarios do not result in fuel damage, but physical aspects of system prevent these scenarios from occurring. It is not possible to achieve full power operation with the pulse rod fully inserted; since the pulse rod is partially withdrawn with air applied to the pulse solenoid, it physically cannot be pulsed. Although not required to ensure the safety of the reactor, an interlock prevents pulsing from power levels greater than a maximum of 10 kW.

c. Conclusions

Insertion of the maximum possible reactivity without initial temperature feedback (i.e., fuel temperature is too low to limit core available reactivity) results in a peak hot spot fuel temperature of 746°C, well below the safety limit.

Insertion of the maximum possible reactivity with initial temperature feedback (i.e., fuel temperature limits available) results in a peak hot spot fuel temperature of 869°C, well below the safety limit.

13.2.4 Single Element Failure in Air

Inventories of radioactive fission products are computed using the Oak Ridge Isotope Generation code (ORIGEN) to support analysis of a maximum hypothetical accident involving cladding failure in a single TRIGA fuel element. A fraction of the radionuclide inventory is postulated to escape from the fuel element to the reactor bay with potential exposure to radiation workers, then to the environment with potential exposure to the general public. The type and quantity of radionuclides released is developed from two limiting cases: long lived radionuclides are based on historical operations, and a different inventory was developed using a high power operating history over a short period. The highest inventory of the radioisotopes calculated for the two cases are assumed to be combined in a single fuel rod in a "reference fuel element."

For historical operations, source terms are computed in a fuel element from continuous operation for 40 years at the average power experienced by the reactor over its first 33 years of operation. The source term is computed for the fuel rod experiencing the maximum power for the average power during the period. Also examined are residual sources still present in fuel, but generated in reactor operations prior to local receipt of the fuel in 1973.

For the short term operations, source terms are computed based on operating 8 hours per day for 5 days prior to fuel element failure. The source term is computed for the fuel rod experiencing the maximum power for the average power level following full power operations as described.

Consequence and dose analysis is provided for two competing conditions. Potential exposure to radiation workers assumes that the radionuclide release is held within the reactor bay. Potential exposure to members of the public assumes unrestricted release of the radionuclides in a plume from the reactor bay exhaust fan. The sum of the ratio of radionuclide activity to the associated Annual Limit on Intake (ALI) for each radionuclide is directly proportional to the dose associated with one ALI; the ALI is used to determine the Derived Air Concentration (DAC). Worker and public doses are calculated based on reactor bay and effluent concentrations of each radionuclide compared to DAC values and effluent limits for the radionuclides.

Although the initial radionuclide release inventory exceeds the Annual Limit on Intake, there is no conceivable means of delivering the total inventory to a single worker. The radionuclide inventory falls below the Annual Limit on Intake at about 97 days. More significantly, based on the distribution of radionuclide inventory in the reactor bay atmosphere and then as released, public and worker doses are calculated to be less than 10CFR20 limits for annual exposure.

a. Assumptions and Approximations

Following are assumptions and approximations applied to calculations.

- Power history prior to cladding failure:
 1. For long-lived radionuclides, calculations of radionuclide inventory in the fuel element are based on continuous operation prior to fuel failure for 40 years at the average thermal power experienced by the reactor during its first 33 years of operation, namely, 3.50 kW.
 2. For short-lived radionuclides,

Calculations of radionuclide inventory in fuel are based on operation at the full thermal power of 1,250 kW for eight hours per day, for five successive days prior to fuel failure, for an average thermal power (P_{AVE}) of:

$$P_{AVE} = 1250 \text{ kW} \cdot \frac{8 \text{ h}}{24 \text{ h}} = 416.67 \text{ kW} \quad (25)$$

The release is assumed to occur 20 minutes after reactor operations is terminated

- Radionuclide inventory in one "worst-case" fuel element is based on 81 elements in the core for the historical period and [redacted] elements for full power operation (the case for core II-16), [redacted] of ^{235}U per element [redacted], and a very conservative value of 2.0 as the ratio of the maximum power produced by a single element in the core to the average power produced per fuel element.

$$P_{eff} = \frac{P_{AVE}}{Rods} \cdot 2.0 \quad (26)$$

Thus, for the historical period, the worst case element has an effective power of:

$$P_{eff} = \frac{3.5 \text{ kW}}{[redacted]} \cdot 2.0 = [redacted] \quad (27)$$

And for the one-week full-power operation the worst case element has an effective power of:

$$P_{eff} = \frac{416.67 \text{ kW}}{[redacted]} \cdot 2.0 = [redacted] \quad (28)$$

- The fraction of noble gases and iodine contained within the fuel that is actually released is 1.0×10^{-4} . This is a very conservative value prescribed in NUREG 2387 [Hawley and Kathren, 1982] and may be compared to the value of 1.5×10^{-5} measured at General Atomics [Simnad et al., 1976] and used in SARs for other reactor facilities [NUREG-1390, 1990].
- The fractional release of particulates (radionuclides other than noble gases and iodine) is 1.0×10^{-6} , a very conservative estimate used by Hawley and Kathren [1982].
- ALI and DAC values include the effects of the ingrowth of daughter radionuclides produced in the body by the decay of the parent (10CFR20, Appendix B, *Notation*, Table 1). Calculation of average concentration for consequence analysis is based on the average (taken by integration and normalization of the radioactive decay formula) over a one-year decay interval.

b. Radionuclide Inventory Buildup and Decay

Consider a mass of ^{235}U yielding thermal power P (kW) due to thermal-neutron induced fission. The fission rate is related to the thermal power by the factor $k = 3.12 \times 10^{13}$ fissions

per second per kW.⁶ Consider also a fission product radionuclide, which is produced with yield Y , and which decays with rate constant λ . It is easily shown that the equilibrium activity A_∞ (Bq) of the fission product, which exists when the rate of creation by fission is equal to the rate of loss by decay, is given by $A_\infty = kPY$. Here it should be noted that the power must be small enough or the uranium mass large enough that the depletion of the ^{235}U is negligible.⁷ Starting at time $t = 0$, the buildup of activity is given by:

$$A(t) = A_\infty * (1 - e^{-\lambda t}) \tag{29}$$

For times much greater than the half-life of the radionuclide, $A \approx A_\infty$, and for times much less than the half-life, $A(t) = A_\infty * \lambda * t$. If the fission process ceases at time t_1 , the specific activity at later time t is given by

$$A(t) = A_\infty * (1 - e^{-\lambda t_1}) * e^{-\lambda(t-t_1)} \tag{30}$$

Consider the fission product ^{131}I , which has a half-life of 8.04 days ($\lambda = 0.00359 \text{ h}^{-1}$) and a chain (cumulative) fission product yield of about 0.031. At a thermal power of 1 kW, the equilibrium activity is about $A_\infty = 9.67 \times 10^{11} \text{ Bq}$ (26.1 Ci). After only four hours of operation, though, the activity is only about 0.37 Ci. For equilibrium operation at 3.5 kW, distributed over 30 fuel elements, the average activity per element would be $26.1 \times 3.5 \div 30 = 3.11 \text{ Ci}$ per fuel element. The worst case element would contain twice this activity. With a release fraction of 1.0×10^{-4} , the activity available for release would be about $3.11 \times 2 \times 1.0 \times 10^{-4} = 6.22 \times 10^{-4} \text{ Ci}$. This type of calculation is performed by the ORIGEN code [CCC-371] for hundreds of fission products and for arbitrary times and power levels of operation as well as arbitrary times of decay after conclusion of reactor operation. The code accounts for branched decay chains. It also may account for depletion of ^{235}U and ingrowth of ^{239}Pu , although those features were not invoked in the calculations reported here because of minimal depletion in TRIGA fuel elements.

c. Data From Origen Calculations

The inventory of radionuclides in 1 tonne of ^{235}U was calculated by ORIGEN for 40 years of continuous operation at 1 watt, and then for 8-hours/day for five consecutive days. The ORIGEN calculations produce 688 radionuclides with non-zero values for the historical activity and 677 radionuclides for the short term operations. The activity values are scaled to the mass of a fuel rod and the average power history for the assumed operation (historical and short term). The maximum activity values for each radionuclide (comparing the two operations) provide the basis for the radionuclide inventory of the reference fuel rod. The inventory of radionuclides generated by ORIGEN at termination of operations is extracted from ORIGEN-2.1 calculation output files, with the ORIGEN based inventory reproduced in Appendix C in the *Historical Ops* and *Short Term Ops* sections, *ORIGEN* columns.

⁶ Note that the product of k and yield Y may be stated as $3.12 \times 10^{13} \times Y \text{ Bq/kW}$ or $843 \times Y \text{ Ci/kW}$.

⁷ Negligible burnup is modeled in ORIGEN calculations by setting the fuel mass very large (1 tonne) and the thermal power very low (1 kW or less).

d. **Radionuclide Release Inventory**

The activity of the fission product inventory (FPI) in Curies is computed by ORIGEN for 1 tonne () of ^{235}U fuel at 1 Watt to simulate fission product inventory buildup with negligible burnup. A fuel rod contains () grams () of ^{235}U (op. cit.); the fission product inventory of a single rod is a fraction () of the inventory calculated by ORIGEN (FPI_{ORIGEN}) at 1 watt. Therefore, the fission product inventory of the worst case fuel rod (FPI_{Rod}) is scaled for power and mass of a single fuel rod:

$$FPI_{Rod} \left[\frac{\mu\text{Ci}}{\text{Rod}} \right] = FPI_{ORIGEN} \left[\frac{10^6 \mu\text{Ci}}{1,000 \text{ kg} \cdot \text{W}} \right] \cdot P_{eff} \cdot \frac{\text{Rod}}{\text{Rod}} \quad (31)$$

$$FPI_{Rod} \left[\frac{\mu\text{Ci}}{\text{Rod}} \right] = \text{Rod} \cdot FPI_{ORIGEN} \cdot P_{eff} \left[\frac{\mu\text{Ci}}{\text{W} \cdot \text{Rod}} \right] \quad (32)$$

For the historical calculation (P_{eff} of 86.4 W), the fuel rod fission product inventory is:

$$FPI_{Rod} \left[\frac{\mu\text{Ci}}{\text{Rod}} \right] = \text{Rod} \cdot FPI_{ORIGEN} \mu\text{Ci} \quad (33)$$

The fission product inventory based on short term operations (P_{eff} of 10.04 kW calculated in 13.2.4.a) is calculated from equation (32):

$$FPI_{Rod} \left[\frac{\mu\text{Ci}}{\text{Rod}} \right] = \text{Rod} \cdot FPI_{ORIGEN} \cdot \mu\text{Ci} \quad (34)$$

ORIGEN identifies an inventory of 688 fission products for the calculation incorporating the extended operating period, and 677 fission products for the short operating period, although the inventory is extremely small for a large fraction of the isotopes. The radionuclide activity (A_x) that escapes the fuel rod is calculated based on release fractions for particulate and gaseous nuclides (given in 13.2.4.a):

Particulate Activity Released

$$A_{particulate} = FPI_{Rod} \left[\frac{\mu\text{Ci}}{\text{Rod}} \right] \cdot 10^{-6} \quad (35)$$

For particulate radionuclides calculated from historical operations, the radionuclide release is calculated:

$$A_{particulate} = 3.37 \cdot 10^{-3} \cdot FPI_{ORIGEN} \mu\text{Ci} \quad (36)$$

For particulate radionuclides calculated from short term operation the radionuclide release is calculated:

$$A_{particulate} = \text{[REDACTED]} \cdot FPI_{ORIGEN} \cdot \mu Ci \quad (37)$$

Noble Gas and Iodine Activity

$$A_{gas} = FPI_{Rod} \left[\frac{\mu Ci}{Rod} \right] \cdot 10^{-4} \quad (38)$$

For iodine and gaseous radionuclides calculated from historical operations, the radionuclide release is calculated:

$$A_{gas} = \text{[REDACTED]} \cdot FPI_{ORIGEN} \mu Ci \quad (39)$$

For noble gas radionuclides calculated from short term operation, the radionuclide release is calculated:

$$A_{gas} = \text{[REDACTED]} \cdot FPI_{ORIGEN} \mu Ci \quad (40)$$

Reference Case Source Terms

The ORIGEN output for each case (Appendix C, *Historical Ops* and *Short Term Ops* sections, *ORIGEN* columns) are corrected for power and fuel mass (Appendix C, *Historical Ops* and *Short Term Ops* sections, *Fuel Rod* columns). The highest value radionuclide from the two cases for a TRIGA fuel element are compared, with greater values for any one isotope selected as reference case source terms for maximum hypothetical accident (Appendix C, *REFERENCE ROD*).

Decay Correction

There is a finite amount of time between shutdown and removal of the fuel from the core during which radionuclides decay. While normal fuel handling practice precludes handling fuel the same day following power operations, a minimum of approximately 20 minutes would be required to initiate fuel handling after operations. The minimum time includes preparing the fuel handling tool, staging the cask, lowering the cask into the pool, grappling and removing the fuel element, transferring the element to the fuel handling cask, and removing the fuel handling cask from the pool prerequisite to the removal of the cladding from the fuel element.

The ORIGEN calculation identifies 685 non-zero value radionuclides. A large fraction of the nuclides (202 out of the total) have half lives short enough that after 20 minutes they are essentially completely decayed. Therefore, the activities calculated were decreased by (indicated in Appendix C tables, *REFERENCE ROD*, column *T=0* for inventory at shutdown and column *20 MIN SRC* for source inventory at 20 minutes):

$$A_{released} = A_{inventory} \cdot e^{-\frac{0.693}{t_{1/2}} \cdot 20 \text{ min}} \quad (41)$$

$$A(0.01389 d^{-1}) = A_0 \cdot e^{-0.01389 d^{-1}} \quad (42)$$

e. Derived Quantities

Regulatory Guideline 8.34, *Monitoring Criteria and Methods To Calculate Occupational Radiation Doses*, provides methodology to determine potential dose rates from ingestion of, or immersion in, radionuclides using data in 10CFR20 Appendix B. If available radionuclide inventory is less than one "Annual Limit on Intake" (ALI), then it is not physically possible to exceed the annual limits for worker exposure. If the available radionuclide release exceeds an ALI, then it is necessary to examine the fraction of the inventory to which individuals will be exposed. The Regulatory Guideline also provides guidance for using a "Derived Air Concentration" (DAC) to determine potential dose rates for workers based on a concentration of radionuclides, such as occurs through releasing the inventory into a volume. In a similar manner, the public dose from effluents can be calculated through comparison of the radionuclide concentration in the release to the "Effluent Limits."

The Appendix C tables, column *REFERENCE ROD*, are activities potentially released from a single worst-case fuel element that has experienced a cladding failure. This activity may itself be compared to the annual limit of intake (ALI) to gauge the potential risk to an individual worker. By dividing the activity by the free volume of the reactor bay in the Nuclear Reactor Facility, one obtains an air concentration (specific activity) that may be compared to the derived air concentration (DAC) for occupational exposure as given 10CFR20 or in EPA federal guidance [Eckerman et al., 1988]. Reducing the concentration of elevated releases, one obtains air concentration that may be compared to the effluent limits of 10CFR20, Appendix B.

The major contributors to the dose for a release 20 minutes after shutdown are tabulated in Appendix C tables, column *REFERENCE ROD*, column *20 MIN*. Appendix D tables identify the ALI, DAC and effluent limits along with the initial inventories.

The tables contain a comparison of the ratios of the reference case releases to the ALI immediately following shutdown and for a release beginning 20 minutes after shutdown. The 20-minute reference case is modified by dilution in the reactor bay environment (for the DAC) and stack release (for the effluent limit) and the stack release further modified for physical characteristics, with the modified releases compared to the appropriate limit.

Consequence Analysis

The ALI is the quantity of radionuclide that, if ingested, will result in either a CEDE of 5 rem or a CDE of 50 rem. Therefore, the potential for radionuclide ingestion R exceeding limiting values in a mixture of radionuclides with activities A_i (where i is a specific nuclide) can be calculated based on the sum of each concentration weighted by the radionuclide ALI value:

$$R = \sum_{i=\text{All nuclides}} \frac{A_i}{ALI_i} \quad (43)$$

The Derived Air Concentration corresponds to the concentration of a radionuclide that will result in 1 ALI for a worker exposed to the radionuclide 40 hours per week for 50 weeks. During the year of exposure, radionuclides decay. The average value of the concentration over the year of exposure is a function of the decay of the radionuclide inventory, and for individual radionuclides is:

$$\bar{C} = \frac{1}{365.25} \cdot \int_0^{365.25} C(t) dt = \frac{C_0}{365.25} \cdot \int_0^{365.25} e^{-\lambda t} dt \quad (44)$$

$$\bar{C} = \frac{C_0}{365.25} \cdot \frac{1 - e^{-\lambda \cdot 365.25}}{\lambda} \quad (45)$$

Therefore the dose (D) received by a worker exposed to a mixture of average radionuclide concentrations (\bar{C}_i , where i is a specific nuclide) can be calculated the sum of each concentration weighted by isotope the DAC (DAC_i) value:

$$D = \left\{ \begin{array}{l} 5 \text{ rem CEDE} \\ 50 \text{ rem CDE} \end{array} \right\} \cdot \sum_{i=\text{All nuclides}} \frac{\bar{C}_i}{DAC_i} \quad (46)$$

Effluent limits (EL) are based on exposure to a radionuclide concentration in airborne effluents that results in a dose of 50 mrem in one year. Hawley and Kathern [1982] use a breathing standard in dose analysis of $1.2 \text{ m}^3 \text{ h}^{-1}$. Although the exhaust system will discharge orders of magnitude greater volumetric rate from the reactor bay, the standad breathing rate will be artificially and conservatively considered as the minimum transport rate for determining physical removal of the source term for effluent release. Assuming a direct path for the radionuclide concentration in the reactor bay exhaust to the receptor with no atmospheric dispersion other than the standard elevated release factor, the removal of a small quantity of radionuclides through inhalation will modify the time dependence of the removal term from the radioactive decay constant to an effective decay constant with an added term, the ratio of the breathing rate to the volume of the reactor bay:

$$\bar{C} = \frac{C_0}{365.25} \cdot \frac{1 - e^{-\left[\lambda + \frac{1.2 \cdot 24}{4078}\right] 365.25}}{\lambda + \frac{1.2 \cdot 24}{4078}} \quad (47)$$

Therefore the dose (D) received by a member of the public exposed to a mixture of average radionuclide concentrations (CE_i , where i is a specific nuclide) can be calculated the sum of each concentration weighted by effluent limit for the nuclide (EL_i) the dose value (50 mrem):

$$D = 50 \text{ mrem} \cdot \sum_{i=\text{All nuclides}} \frac{CE_i}{EL_i} \quad (48)$$

10CFR20 (Appendix B) lists ALI, DAC and Effluent Limits for (a group of) specific activities and establishes standard values for nuclides not listed. The reference rod inventories of radionuclides are tabulated in Appendix D with the associated ALI, DAC and Effluent Limits.

Release Inventory Compared to Derived Quantities

Appendix D is a set of tables tabulating nuclides identified in ORIGEN, 10CFR20 limits, radionuclide inventory at shutdown, radionuclide inventory 15 minutes following shutdown (when cladding failure is assumed to initiate), and the weighted fractions of each limit

associated with each nuclide. The sum of the weighted values is presented in Table 13.10 for (1) particulate radionuclides listed in 10CFR20 Appendix B, (2) particulate nuclides present in the ORIGEN calculations but not specifically listed in 10CFR20, (3) gaseous radionuclides listed in 10CFR20 Appendix B, and (4) gaseous nuclides present in the ORIGEN calculations but not specifically listed in 10CFR20.

The weighted average of each radionuclide to its associated ALI at time of shutdown and 20 minutes later, when the cladding failure occurs, is presented in Table 13.10. Figure 13.4 illustrates how the ratio declines in time the release inventory decays. After 97 days, the ratio is less than unity illustrating that limiting access in combination with a substantial decay period prior to entry with extended access in the reactor bay following release is an effective way to assure worker exposures remain within annual limits.

Table 13.10, Summary of Ratios, Values: Limits

Nuclide Characterization	ALI		DAC	EFF LIMIT
	T=0	20 MIN	ANN AVE	ANN AVE
Gaseous in 10CFR20	1.97E0	1.93E0	2.57E-2	1.17E-2
Gaseous not listed	3.79E1	3.48E-2	9.75E-7	1.95E-6
Particulates in 10CFR20	7.03E0	6.66E0	5.22E-1	1.80E-1
Particulates not listed	4.43E2	3.26E1	1.00E-2	1.99E-2
TOTALS	4.90E2	4.12E1	5.57E-1	2.11E-1
CORRESPONDING DOSE (R h ⁻¹)	2.45E3	2.06E2	2.79E0	1.06E-2

ALI Ratio vs Time for MHA

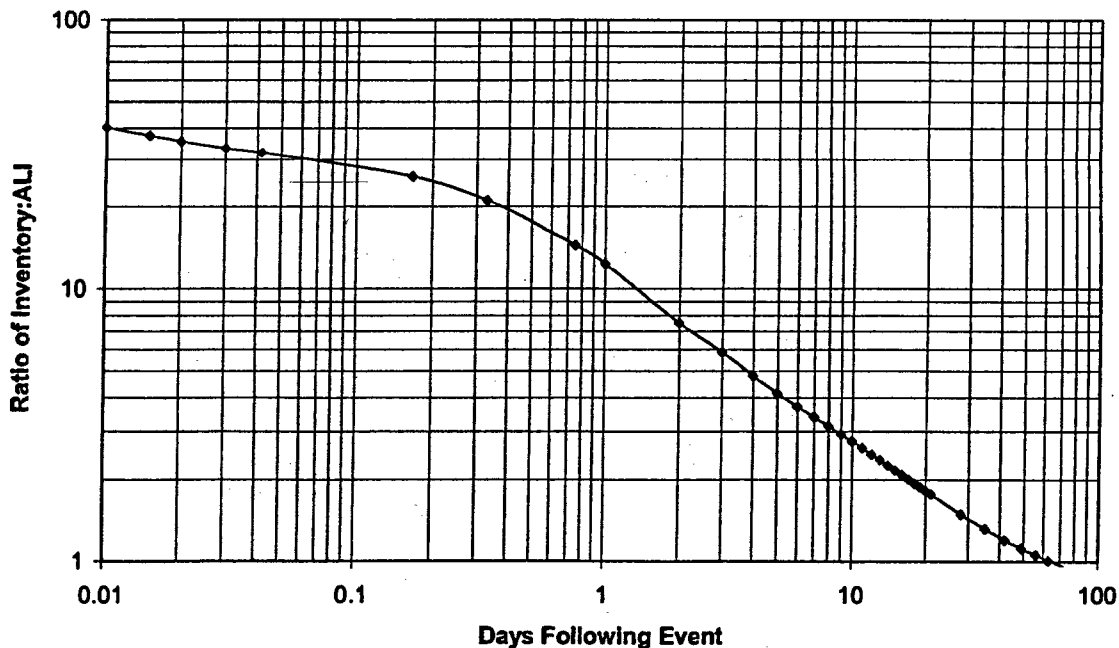


Figure 13.4, ALI Ratio Variation in Time

Although radionuclide inventory exceeds the amount that can be ingested and not exceed limiting values of 10CFR20 for 97 days following cladding failure, there is no physically credible scenario through which all available radionuclide can be ingested by an individual; the high ALI ratios indicate the necessity for further analysis of possible worker doses. Therefore, consequence analysis based on the Derived Air Concentration and Effluent Limit values of 10CFR20 Appendix B follows.

The resulting sum of the weighted average of the ratio of radionuclide concentrations to their associated DAC values using equations (45) and (46) is provided in Table 13.10. The dose to an individual who works within the reactor bay following cladding failure (with the assumed release fractions) for 50 weeks in 40 hour work-weeks if the radionuclides are trapped and mixed within the reactor bay atmosphere for the duration (also provided in the table) is within annual exposure limits for radiation workers in 10CFR20. This is extremely conservative in assuming continuous exposure (whereas reactor bay entry following an accident will be tightly controlled) and no mitigating action to limit the concentration of airborne radionuclides (such as filtered ventilation).

Similarly, the sum of the weighted average of the ratio of radionuclide concentrations in gaseous effluent to their associated effluent limit using equations (47) and (48) is provided in Table 13.10. The dose received by a member of the public exposed to a plume at the calculated concentration of the specified radionuclides (also provided in the table) is shown to be less than the limit on annual public exposures from licensed activities, although 6% greater than the limit exposure from normal operations. This analysis is extremely conservative in assuming continuous exposure in a controlled area, no mitigating action to limit the concentration of airborne radionuclides in the reactor bay, and no physical removal of radionuclides except via breathing by the affected member of the public.

In addition, Regulatory Guideline 8.34 permits disregarding radionuclides in a mixture under conditions that (1) the radionuclide concentration is less than 10% of the associated DAC, (2) the sum of the ratios of all disregarded radionuclides does not exceed 30%, and (3) total activity is used in demonstrating compliance with dose limits and monitoring requirements. The maximum ratio of any radionuclide in the effluent analysis is less than 10%, and only eight radionuclides have ratios (radionuclide concentration to effluent limit) greater than 0.5%. The eight radionuclides account for 16.7% of the total effluent ratio indicated in Table 13.10, with a corresponding dose of 8.3 mrem.

Summary

A worker who spends one year working in the reactor bay if the radionuclides were trapped in the reactor bay would not exceed the annual limit for normal operations.

If the postulated release from the fuel rod is released from the reactor bay at concentrations based on initial inventory and decay characteristics of the radionuclides for one year, a member of the public exposed to the reactor exhaust plume would not exceed the public exposure limit for normal operations of 100 mrem in a year. Although (when considering the contribution from all radionuclides) the dose attributable to gaseous effluent is slightly higher than the 10 mrem exposure from stack releases permitted for normal operations, disregarding minor contributors as allowed by Regulatory Guideline 8.34 lowers the dose well below the 10 mrem limit for normal operations.

i. **Residual Activity from Fuel Utilization Prior to Receipt**

All but a few instrumented Mark-II fuel elements in the original 1962 core loading were replaced by Mark-III elements on July 10, 1973. The replacement elements had seen considerable use prior to their installation at Kansas State University. The two most heavily used elements, with serial numbers 4078 and 4079, had experienced, respectively, consumption of 11.27 and 10.33 g of ^{235}U . Even after about 25 years of subsequent use, considerable ^{137}Cs , ^{90}Sr , and ^{85}Kr remain from fission during the pre-1973 use. However, the ^{85}Kr atmospheric concentration inside the reactor bay immediately after release would be orders of magnitude lower than the DAC. Therefore only ^{37}Cs and ^{90}Sr offer a potential for occupational or public risk. In the absence of knowledge about the pattern of early fuel utilization, it is assumed that all the generation of fission products took place in 1973 and that fission product decay took place over the period of 28 years from 1973 until 2001.

If Y is the fission yield, λ is the decay constant (s^{-1}), and N_a is Avogadro's number, the activity A (Bq) of any one radionuclide immediately after fissioning of mass m (g) of ^{235}U is

$$A = \frac{N_a}{235} m Y \lambda. \quad (49)$$

Activity calculations using this formula and consequences are reported in Table 13.12.

Table 13.12. Worst Case Source Terms and Consequence Calculations for a Single TRIGA Fuel Element Experiencing 11.27 g of ^{235}U Consumption 28 Years Prior to Element Failure.

FACTOR	RADIONUCLIDE	
	^{90}Sr	^{137}Cs
Half life (y)	29.12	30.00
Decay constant λ (s^{-1})	7.54×10^{-10}	7.32×10^{-10}
Fission yield Y	0.0577	0.0615
Release fraction	1.00×10^{-06}	1.00×10^{-06}
Initial Bq/g contained in element	[REDACTED]	[REDACTED]
Initial μCi available for release	[REDACTED]	[REDACTED]
μCi available for release in 28 y	[REDACTED]	[REDACTED]
ALI (μCi)	[REDACTED]	[REDACTED]
Reactor bay concentration ($\mu\text{Ci}/\text{cm}^3$)	[REDACTED]	[REDACTED]
DAC ($\mu\text{Ci}/\text{cm}^3$)	[REDACTED]	[REDACTED]
Tissue at risk	Bone surface	Total body
Dose conversion factor (mrem/ μCi)	[REDACTED]	[REDACTED]
Maximum downwind dose (mrem)	0.16	0.0020

Whereas the ^{90}Sr activity available for release would exceed the occupational ALI and, if dispersed within the reactor bay, would have a concentration in excess of the DAC, credible mechanisms for ingestion or inhalation of the full available activity or even its full dispersion are not apparent. Thus, neither the ^{90}Sr nor the ^{137}Cs would pose a significant occupational threat. Even if the total available activity were somehow dispersed to the free atmosphere, no person downwind of the accidental release would receive doses even approaching regulatory limits.

j. Conclusions

Fission product inventories in TRIGA fuel elements were calculated with the ORIGEN code, using very conservative approximations. Then, potential radionuclide releases from worst-case fuel elements were computed, again using very conservative approximations. Even if it were assumed that releases took place immediately after reactor operation, and that radionuclides were immediately dispersed inside the reactor bay workplace, few radionuclide concentrations would be in excess of occupational derived air concentrations, and then only for a matter of hours or days. Only for certain nuclides of iodine would the potential release be in excess of the annual limit of intake. However, there is no credible scenario for accidental inhalation or ingestion of the undiluted radioiodine that might be released from a damaged fuel element.

For the residual ^{90}Sr and ^{137}Cs remaining in fuel elements from consumption of ^{235}U prior to receipt of the fuel at Kansas State University, only the former would pose any conceivable occupational threat. However, the total ^{90}Sr activity available for release is estimated to be at most about 4 times the ALI and there is no credible scenario for its consumption by a worker.

As far as potential consequences to the general public are concerned, only for the few radionuclides listed in Table 13.14, are maximum concentrations inside the reactor facility in excess of effluent concentrations listed in 10CFR20 and potential doses 0.001 mrem or greater. However, even in the extremely unlikely event that radionuclides released from a damaged fuel element were immediately released to the outside atmosphere, very conservative calculations reveal that radionuclides inhaled by persons downwind from the release would lead to organ doses or effective doses very far below regulatory limits. As is shown in Table 13.15, the same is true for residual ^{90}Sr and ^{137}Cs remaining in fuel elements from early operations.

13.3 Bibliography

ANSI/ANS-5.1-1994, "American National Standard for Decay Heat Power in Light Water Reactors," American Nuclear Society, 1994.

Report LA-12625-M, Version 4B, "MCNP-- A General Monte Carlo N-Particle Transport Code," Los Alamos National Laboratory, Los Alamos, NM (1997). Briesmeister, J.F. (ed),

CCC-371, "ORIGEN 2.1 Isotope Generation and Depletion Code: Matrix Exponential Method," Radiation Shielding Information Center, Oak Ridge National Laboratory, Oak Ridge, Tennessee, 1991.

Kansas State University TRIGA MkII Reactor Hazards Summary Report, License R-88, Docket 50-188 , (1961) Clack, R.W., J.R. Fagan, W.R. Kimel, and S.Z. Mikhail.,

"Laminar-Flow Heat Transfer for In-Line Flow Through Unbaffled Rod Bundles," Nucl. Sci. Engg. 42, 81-88 (1970), Dwyer, O.E. and H.C. Berry.

"Nuclear Heat Transport," International Textbook Company, Scranton, 1971, El-Wakil, M.M.,

Federal Guidance Report No. 11, Report EPA-5201/1-88-020, U.S. Environmental Protection Agency, *"Limiting Values of Radionuclide Intake and Air Concentration and Dose Conversion Factors for Inhalation, Submersion, and Ingestion,"* Washington, DC, (1988), Eckerman, K.F., A.B. Wolbarst, and A.C.B. Richardson.

Report LA-5885-MS "CINDER-7: An Interim Report for Users,, England, T.R., et al., Los Alamos Scientific Laboratory, Los Alamos, NM, 1976.

"Radiological Assessment," Prentice Hall, Englewood Cliffs, N.J., 1993, Faw, R.E., and J.K. Shultis. *Report LA-9362, "Application of Adjusted Data in Calculating Fission Produce Decay Energies and Spectra,"* Los Alamos Scientific Laboratory, 1982. George, D.C., R.J. LaBauve, and T.R. England.

NUREG/CR-2387 (PNL-4028), "Credible Accident Analyses for TRIGA and TRIGA-Fueled Reactors," Report Pacific Northwest Laboratory, Richland Washington, 1982., Hawley, S.C., and R.L. Kathren,

"Fundamentals of Heat and Mass Transfer," 3d ed., Wiley, New York, 1990, Incropera, F.P. and D.P. DeWitt,

GA-3399, KSU TRIGA Reactor Mechanical Maintenance and Operating Manual, General Atomics Report, 1962.

"Fission Product Analytical Source Functions," Nuclear Technology 56, 332-339 (1982). LaBauve, R.J., T.R. England, and D.C. George, See also Reports LA-9090-MS (1981) and LA-UR-80-3305 (1980), Los Alamos Scientific Laboratory, Los Alamos, NM.

Metals Handbook, 8th ed., Vol. 1, American Society for Metals, Metals Park, Ohio, 1961.

NUREG-1282, "Safety Evaluation Report on High-Uranium Content, Low-Enriched Uranium-Zirconium Hydride Fuels for TRIGA Reactors," Office of Nuclear Reactor Regulation, U.S. Nuclear Regulatory Commission, 1987.

NUREG-1390, "Safety Evaluation Report Relating to the Renewal of the Operating License for the TRIGA Training and Research Reactor at the University of Arizona," Report NUREG-1390, Office of Nuclear Reactor Regulation, U.S. Nuclear Regulatory Commission, 1990.

NUREG-1537, "Guidelines for Preparing and Reviewing Applications for the Licensing of Non-Power Reactors, Format and Content," Report NUREG-1537 Part 1, Office of Nuclear Reactor Regulation, U.S. Nuclear Regulatory Commission, 1996.

"The U-Zr-Hx Alloy: Its Properties and Use in TRIGA Fuel," Report E-117-833, Simnad, M.T, General Atomics Corp., 1980.

"Fuel Elements for Pulsed TRIGA Research Reactors," Nuclear Technology 28, 31-56 (1976) Simnad, M.T., F.C. Faushee, and G.B. West

"Longitudinal Laminar Flow Between Cylinders Arranged in a Regular Array," *AIChE Journal* 5, 325 (1959), Sparrow, E.M., and A.L. Loeffler, and H.A. Hubbard.

Nuclear Systems I: Thermal Hydraulic Fundamentals, Todreas, N.E. and M.S. Kazimi, Hemisphere, New York, 1990.

Safety Analysis Report, TRIGA Reactor Facility, Nuclear Engineering Teaching Laboratory, University of Texas at Austin, Revision 1.01, Docket 50-602, May, 1991.

"Kinetic Behavior of TRIGA Reactors," Report GA-7882, West, G.B., W.L. Whittemore, J.R. Shoptaugh, Jr., J.B. Dee, and C.O. Coffer, , General Atomics Corp., 1967.

APPENDICES TO CHAPTER 13

- A. MCNP Model for Loss of Pool Water Dose Analysis
- B. Origen 2.1 input files
 - i. ^{235}U fission at 1 W thermal power for 40 years.
 - ii. ^{235}U fission at 1 W thermal power 8 hours per day for 5 days
- C. Tabulated Source Term Values
- D. Consequence Analysis

**The Appendices have been
Redacted as Security
Related Sensitive
Information**